

SBA-15 Supported Fe, Ni, Fe-Ni Bimetallic Catalysts for Wet Oxidation of Bisphenol-A

Suranjana V. Mayani, Vishal J. Mayani, and Sang Wook Kim*

Department of Advanced Materials Chemistry, College of Science and Technology, Dongguk University, Gyeongbuk 780-714, Korea. *E-mail: swkim@dongguk.ac.kr
Received July 23, 2014, Accepted August 18, 2014

Bisphenol A is considered as pollutant, because it is toxic and hazardous to living organisms even at very low concentrations. Biological oxidation used for removing this organic from waste water is not suitable and consequently application of catalytic wet oxidation has been considered as one of the best options for treating bisphenol A. We have developed **Fe/SBA-15**, **Ni/SBA-15** and **Fe-Ni/SBA-15** as heterogeneous catalysts using the advanced impregnation method for oxidation of bisphenol A in water. The catalysts were characterized with physico-chemical characterization methods such as, powder X-ray diffraction (PXRD), FT-IR measurements, N₂ adsorption-desorption isotherm, thermo-gravimetric analysis (TGA), scanning electron microscopy (SEM), transmission electron microscopy (TEM) and inductively coupled plasma optical emission spectroscopy (ICP-OES) analysis. This work illustrates activity of the catalysts for heterogeneous catalytic degradation reaction revealed with excellent conversion and recyclability. The degradation products identified were not persistent pollutants. GC-MS analysis identified the products: 2,4-hexadienedioic acid, 2,4-pentadienic acid and isopropanol or acetic acid. The leachability study indicated that the catalysts release very little metals to water. Therefore, the possibility of water contamination through metal leaching was almost negligible.

Key Words : Bisphenol A, Catalytic degradation, Heterogeneous catalysts, Leachability study, Wet oxidation

Introduction

Bisphenol A (BPA) has received great attention as an intermediate chemical in the manufacturing of polycarbonate plastic, epoxy resin, polyester-styrene resins.^{1,2} BPA is manufactured in high quantities, for production of powder paints, adhesives, building materials, compact disks, thermal paper and paper coatings. Due to the daily use of these products, high concentrations of BPA are observed in wastewater. During the manufacturing process, some BPA can be unintentionally released into the environment. BPA has biological toxicity³ and estrogenic activity⁴ toward aquatic organisms and human cultured cells. BPA is considered as pollutant, because it is toxic and hazardous to living organisms, even at very low concentrations. Therefore, it is necessary to develop efficient treatment methodology for the removal of BPA in wastewater. Wastewater treatment methods like chemical precipitation, activated carbon adsorption and ion exchange are typically useful in the removal of bisphenol A.⁵⁻⁷ But, they transfer the contaminants from one medium to another and hence further treatment is required. Hence, a rapid, simple and economic wastewater treatment for the removal of BPA is now highly in demand.

The conventional pollutant destructive technologies include biological, thermal and physico-chemical treatments.⁸ Biological treatments normally require a long time for microorganisms to degrade the pollutant because they are affected by bisphenol A toxicity, thermal treatments produce considerable emissions of other harmful compounds and physico-chemical techniques, such as flocculation, precipitation,

adsorption on activated carbon and reverse osmosis, require a post treatment to remove the pollutant from a newly polluted environment.⁹ Alternative methods to these well established techniques are advanced oxidation processes,¹⁰ which have been reported to be useful for the near ambient degradation of soluble organic contaminants from water and soil providing almost total degradation.

Mesoporous materials (SBA-15, MCM-41 *etc*) have attracted considerable attention in the field of catalysis and adsorption owing to their characteristic properties such as, high surface area, large pore volume, regular structure, uniform pore size distribution and relatively high thermal stability.¹¹⁻¹⁴ SBA-15 has better mechanical and hydrothermal stability than MCM-41.¹² On the other hand, it is very difficult to introduce other metal ions directly into the SBA-15 framework because of the strong acidic conditions for SBA-15 synthesis.^{12,15} Recently, several researchers reported the incorporation of hetero atoms, such as Al, Fe, Co, Ni, Cr and Ti, into the framework of SBA-15 by modifying the pH and/or the hydrothermal method of preparation.¹⁶⁻¹⁹ Fe₂O₃/SBA-15 nano composites, titania-deposited SBA-15, crystalline iron oxide supported on meso-structured SBA-15 materials, Fe/SBA-15 have been applied to waste water treatment processes.²⁰⁻²³ The use of a solid catalyst offers the further advantages of easy recovery, regeneration and reuse, compared to a homogeneous catalyst.²⁴

In the present work, bisphenol A (BPA) is adopted as a model compound to evaluate the wet catalytic oxidation by transition metal supported catalysts (**Fe/SBA-15**, **Ni/SBA-15** and **Fe-Ni/SBA-15**). The effects of reaction time, temper-

ature and leachability study of the catalysts were examined under a range of reaction conditions. The products of the reaction were determined with the help of gas chromatography-mass spectrometry (GC-MS) analysis. Recyclability of the catalyst was also examined.

Experimental

Materials. Poly(ethylene glycol)-block-poly(propylene glycol)-block-poly(ethylene glycol) (P123; Aldrich, USA), hydrochloric acid (Matsunoen Chemicals Ltd., Japan), tetraethyl orthosilicate (TEOS; Aldrich, USA), ferric nitrate nonahydrate (Yakuri pure Chemicals Co. Ltd, Japan) and nickel nitrate hexahydrate (Samchun Pure Chemicals Co. Ltd., Pyongtack city, Kyung ki-do, Korea) were used as received. The reactions were carried out with bisphenol A (Junsei Chemicals Co. Ltd, Japan), H₂O₂ (Wako pure chemicals Industries Ltd., Japan) and stock solution of reactant at 5×10^{-4} M (mol L⁻¹) concentrations was prepared in double distilled water.

Characterization and Measurement. The catalysts were characterized by powder X-ray diffraction (PXRD, Phillips X'pert MPD diffractometer, Almelo, The Netherlands) over the 2 θ range (1–10 and 10–80). Fourier transform infrared (FT-IR, Perkin-Elmer Spectrometer, Massachusetts, USA) spectroscopy was carried out using a KBr self-supported pellet technique. The metals entering into the SBA-15 catalysts were determined by inductively coupled plasma-optical emission spectroscopy (ICP-OES, JY Ultima 2CHR). The BET surface area was completed by N₂ adsorption-desorption data measured at 77 K using a volumetric adsorption set up (Micromeritics ASAP-2010, USA). The pore diameter of the samples was determined from the desorption branch of the nitrogen adsorption isotherm employing the Barret-Joyner-Halenda (BJH) model. The thermal measurements and microstructural evaluation of these samples were examined by thermo-gravimetric analysis (TGA, SDT600, TA instrument, USA), scanning electron microscopy (SEM, LEO-1430, VP, UK) and transmission electron microscopy (TEM, JEM 2011, Jeol Corporation, Japan).

Synthesis of Fe/SBA-15. SBA-15 was synthesized by a hydrothermal crystallization method as described previously.^{12,15,16} Briefly, 4.0 g P123 was dispersed in 30 g of distilled water and stirred for 3h, to the resulting solution 120 g of 2 N HCl was added under stirring and finally 9.5 mL of TEOS was added drop wise as silica source. The mixture was continuously stirred at 313 K for 24 h, then transferred into a teflon-lined autoclave and aged for 48 h at 313 K. The product was filtered, washed and dried at 383 K in air. The obtained sample was calcined at 823 K in air for 6 h; Yield: 6.3 g. **Fe/SBA-15** sample was prepared by wet impregnation using Fe(NO₃)₃·9H₂O as iron precursor. Equal amount of Fe(NO₃)₃·9H₂O (1 g) and SBA-15 (1 g) were dissolved in minimum volume of deionized water (10 mL) under stirring condition for 60 min. The mixture was dried at 353 K, calcined in air at 823 K for 3 h, and obtained **Fe/SBA-15**; Yield: 1.9 g. The dried material was ground well and sieved

using 400 mesh (0.037 mm) size test sieves. FTIR (KBr) ν : 457, 695, 790, 960, 1079, 1229, 1380, 1446, 1635, 1638, 2340, 3436 cm⁻¹. ICP analysis of **Fe/SBA-15** catalyst showed 11.8 wt % iron metal.

Synthesis of Ni/SBA-15. **Ni/SBA-15** sample was prepared by using Ni(NO₃)₂·6H₂O as nickel precursor. In wet impregnation method, equal amount of Ni(NO₃)₂·6H₂O (1 g) and SBA-15 (1 g) were mixed in minimum volume of deionized water (10 mL) under stirring condition for 1 h. The mixture was dried at 353 K, calcined in air at 823 K for 3 h and **Ni/SBA-15** was obtained; Yield: 1.9 g. The dried material was ground well and sieved using 400 mesh (0.037 mm) size test sieves. FTIR (KBr) ν : 803, 1369, 1425, 1461, 1637, 1699, 3464 cm⁻¹. ICP analysis of **Ni/SBA-15** catalyst showed 15.3 wt % nickel metal.

Synthesis of Fe-Ni/SBA-15. **Fe-Ni/SBA-15** sample was prepared by using Fe(NO₃)₃·9H₂O as iron and Ni(NO₃)₂·6H₂O as nickel precursors. In wet impregnation method, Fe(NO₃)₃·9H₂O (1g), Ni(NO₃)₂·6H₂O (1g) and of SBA-15 (2 g) were mixed in 30 ml of deionized water under stirring condition for 1 h. The mixture was dried at 353 K, calcined in air at 823 K for 3 h and **Fe-Ni/SBA-15** was obtained; Yield: 3.9 g. The dried material was ground well and sieved using 400 mesh (0.037 mm) size test sieves. FTIR (KBr) ν : 484, 799, 987, 1085, 1836, 2030, 3448 cm⁻¹. ICP analysis of **Fe-Ni/SBA-15** catalyst showed 4.9 wt % iron and 7.2 wt % nickel metal.

Catalytic Wet Oxidation of Bisphenol A. Catalytic oxidation was carried out in a batch reactor equipped with a condenser under atmospheric pressure. After the reaction was over, mixture was centrifuged and the reactants remaining unconverted were estimated by spectrophotometer (Varian, Cary-4000, USA). Calibration curves obtained with a minimum of 5 standards were used for quantification of the results. The total conversion of bisphenol A was computed from the decrease in concentration of bisphenol A. The percentage conversion is calculated according to the relation:

$$\text{Conversion (\%)} = [(C_0 - C_t)/C_0] \times 100 \quad (1)$$

Where C₀ is the initial concentration (mol L⁻¹), C_t the concentration at any time after the reaction starts, t the time (min). Gas chromatography-mass spectrometry (GC-MS, Shimadzu GC 2010, USA) was used for product identification.

Results and Discussion

Physico-chemical Characterization.

Powder X-ray Diffractions (PXRD) Analysis: The powder X-ray diffraction was used to characterize the crystalline structure of the catalysts. PXRD patterns of SBA-15 showed characteristic low angle peaks at $2\theta = 0.95^\circ, 1.59^\circ, 1.83^\circ$. The hexagonal lattice with the major peak assigned to the reflection from the (100) plane and two minor peaks with lower intensity corresponding to reflections from the (110) and (200) planes^{12-13,15} were observed. Upon functionaliza-

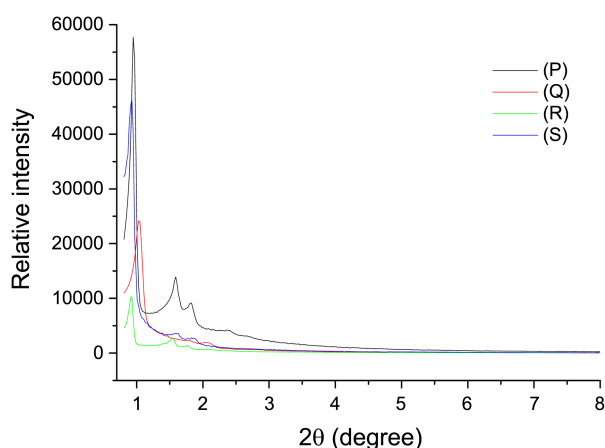


Figure 1. Low angle Powder XRD of SBA-15 (P), Fe/SBA-15 (Q), Ni/SBA-15 (R) and Fe-Ni/SBA-15 (S).

tion of SBA-15 with inorganic metals (Fe, Ni and Fe-Ni bimetallic), the intensity of all the peaks decreased marginally with a small shift in the 2θ values. XRD peaks were observed at $2\theta = 1.03^\circ, 1.45^\circ, 1.81^\circ$ (Fe/SBA-15), $0.93^\circ, 1.55^\circ, 1.77^\circ$ (Ni/SBA-15) and $0.93^\circ, 1.59^\circ, 1.87^\circ$ (Fe-Ni/SBA-15), respectively (Figure 1Q, R, S). This might be due to the presence of metal inside the pores, which causes an increase in the scattering power within the pores, resulting in an overall loss of intensity due to phase cancellation between the pore walls and guest metal.^{13,14,23,25} In high angle PXRD, the existence of major reflections corresponding to SBA-15, even after functionalization, shows that the mesoporous SBA-15 structure is retained (Figure 2). Additionally, there was a broad peak ($2\theta = 23.32^\circ$) attributed to SiO₂ (the component of SBA-15).¹⁴ High angle XRD peaks at $2\theta = 25.49^\circ, 39.35^\circ, 42.27^\circ$ (Fe/SBA-15), $25.93^\circ, 32.76^\circ, 37.84^\circ, 54.19^\circ, 64.67^\circ, 67.96^\circ$ (Ni/SBA-15) and $20.47^\circ, 42.65^\circ, 44.45^\circ, 52.25^\circ$ (Fe-Ni/SBA-15) were observed for metal supported catalyst. Although the catalysts Fe/SBA-15 and Fe-Ni/SBA-15 contain iron metal, the catalysts are not resemble with Fe₂O₃ on mesoporous silica surface as described in high angle XRD (10-80 range). It clearly

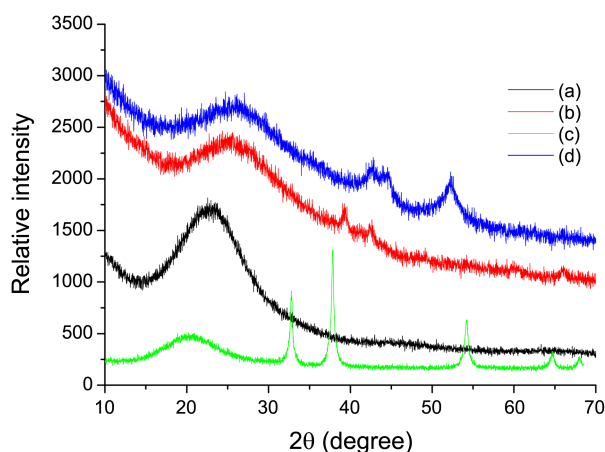


Figure 2. High angle Powder XRD of SBA-15 (a), Fe/SBA-15 (b), Ni/SBA-15 (c) and Fe-Ni/SBA-15 (d).

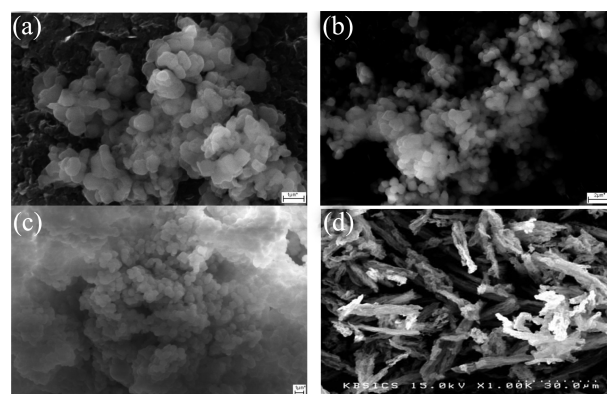


Figure 3. SEM images of SBA-15 (a), Fe/SBA-15 (b), Ni/SBA-15 (c) and Fe-Ni/SBA-15 (d).

suggested that Fe/SBA-15 and Fe-Ni/SBA-15 retained a highly ordered structure of SBA-15 after metal incorporation. There were no obvious diffraction peaks of Fe₂O₃ on mesoporous silica in the wide angle range of the catalysts. Iron species was well dispersed over SBA-15 surface.²⁶ High angle PXRD pattern of the Ni/SBA-15 sample displayed the characteristic peaks corresponding to nickel oxide, too.^{14,27}

Scanning Electron Microscopy (SEM) Analysis and Transmission Electron Microscopy (TEM) Analysis. SEM micrographs showed that the SBA-15 (Figure 3(a)) samples consisted of small agglomerates. The morphology was maintained after metal impregnation to form Fe/SBA-15, Ni/SBA-15 and Fe-Ni/SBA-15 (Figure 3(b), (c), (d)). The catalysts revealed uniform size particles with ordered hexagonal mesoporous structure.^{23,28} TEM micrographs of siliceous SBA-15 confirmed hexagonally arranged pore structures when viewed along the pore direction and parallel lattice

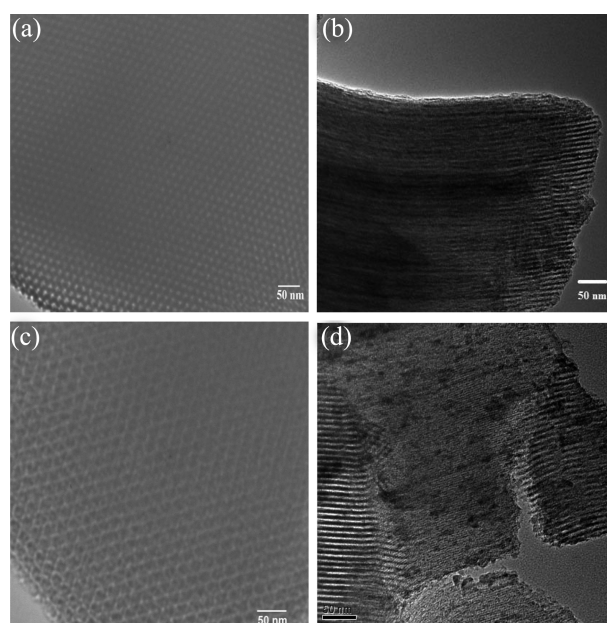


Figure 4. TEM images of SBA-15 (a), Fe/SBA-15 (b), Ni/SBA-15 (c) and Fe-Ni/SBA-15 (d).

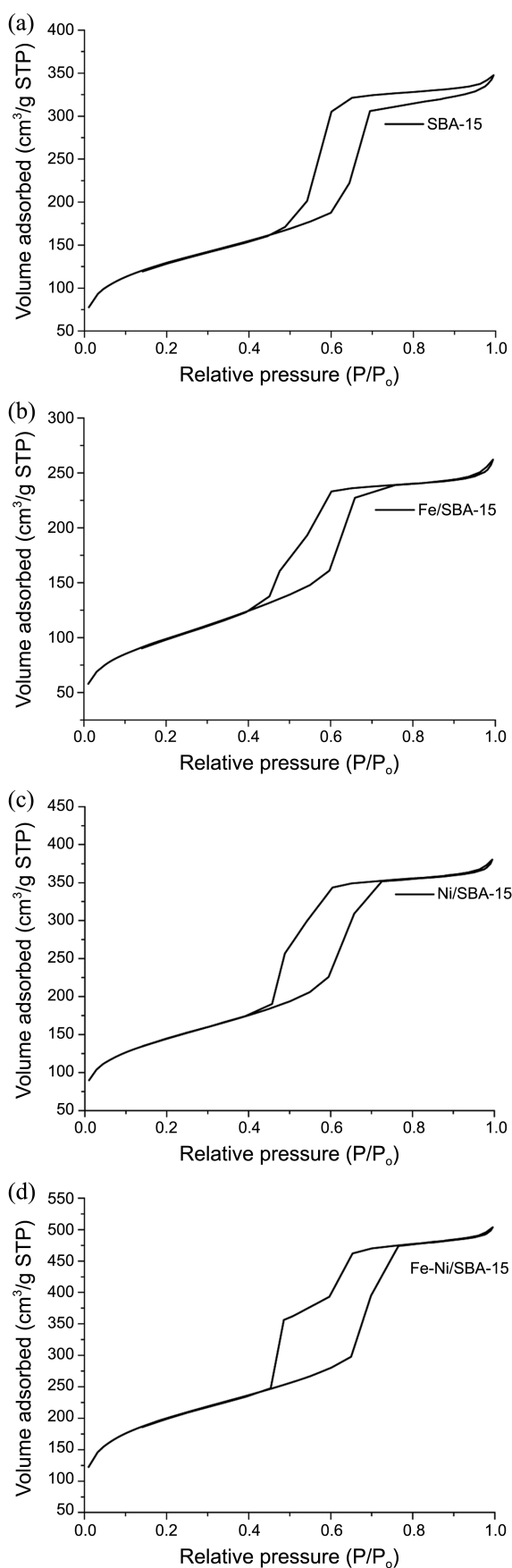


Figure 5. N_2 adsorption-desorption isotherms of SBA-15 (a), Fe/SBA-15 (b), Ni/SBA-15 (c) and Fe-Ni/SBA-15 (d).

Table 1. Surface and pore characteristics of SBA-15, Fe/SBA-15, Ni/SBA-15 and Fe-Ni/SBA-15

Compound	BET surface area (m^2/g)	Total pore volume (cm^3/g)	BJH pore diameter (\AA)
SBA-15	795	1.289	78.9
Fe/SBA-15	512	0.925	73.8
Ni/SBA-15	514	0.568	44.3
Fe-Ni/SBA-15	728	0.760	41.7

fringes when viewed along the side (Figure 4(a)). SBA-15 synthesized in the acidic medium displayed mesopores of one-dimensional channels, indicating SBA-15 to possess a 2D p6mm hexagonal structure. The presence of equidistant parallel fringes exhibits the nature of separation between the layers and the unique well-packed arrangement of mono layers. The ordered mesoporous structure of SBA-15 was unaffected by the incorporation of the metals, as shown in Fe/SBA-15, Ni/SBA-15 and Fe-Ni/SBA-15 (Figure 4(b), (c), (d)).

Nitrogen Adsorption-desorption Isotherm Study. The N_2 adsorption-desorption isotherms of SBA-15 and as prepared catalysts Fe/SBA-15, Ni/SBA-15 and Fe-Ni/SBA-15 showed type IV (Figure 5), which revealed the presence of ordered structure of SBA-15.²⁸⁻³⁰ The Surface and pore characteristics data are summarized in Table 1. A large decrease in BET surface area was observed (from 795 to 512 m^2/g) upon Fe metal functionalisation on SBA-15. Similarly, a decrease in the mesoporous diameter and pore volume from 79 to 74 \AA and 1.289 to 0.925 cm^3/g , respectively, was also observed (Table 1). Decreases in the BET surface area, pore diameter and pore volume from 795 to 514 m^2/g , 79 to 44 \AA and 1.289 to 0.568 cm^3/g , respectively were observed upon Ni incorporation in SBA-15 (Table 1). Whereas for Fe-Ni/SBA-15, BET surface area, pore diameter and pore volume decreased from 795 to 728 m^2/g , 79 to 42 \AA and 1.289 to 0.760 cm^3/g , respectively.

Catalytic Oxidation of Bisphenol A.

Blank Experiments: Before examining the efficiency of the catalysts for the catalytic oxidation of bisphenol A, a set of blank experiments were carried out under the reaction conditions: (i) bisphenol A (5×10^{-4} mole L^{-1}) without a catalyst and H_2O_2 , (ii) bisphenol A (5×10^{-4} mole L^{-1}) and H_2O_2 (1:1 molar ratio) without a catalyst, (iii) bisphenol A (5×10^{-4} mole L^{-1}) with SBA-15 as the catalyst (2 g L^{-1}), and (iv) bisphenol A (5×10^{-4} mole L^{-1}) and H_2O_2 (1:1 molar ratio) with SBA-15 as the catalyst (2 g L^{-1}). The reactions were carried out at 298 K, atmospheric pressure, 200 rpm stirring and a time interval of 2 h. No measurable conversion could be detected for blank experiment.

Effect of the Reaction Time: An increase in the reaction time from 10 to 120 min showed enhanced bisphenol A degradation, as shown in Figure 6. In a series of reactions, which were carried out in this time interval with bisphenol A (5×10^{-4} mole L^{-1}) and H_2O_2 (5×10^{-4} mole L^{-1}) at 298 K using Fe/SBA-15, Ni/SBA-15 or Fe-Ni/SBA-15 as catalyst

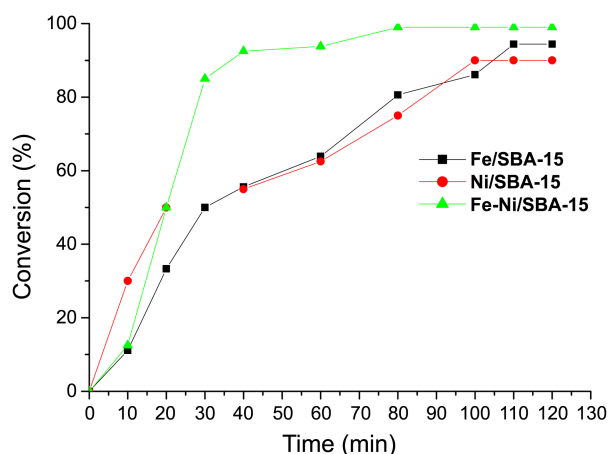


Figure 6. Effects of reaction time on catalytic oxidation of bisphenol A with **Fe/SBA-15**, **Ni/SBA-15** and **Fe-Ni/SBA-15** (load 2 g L^{-1} , bisphenol A: $5 \times 10^{-4} \text{ mole L}^{-1}$) at 298 K.

with a load of 2 g L^{-1} , the conversion increased from 11.1 to 94.4%, 30.0 to 90.0% and 12.5 to 99.0%, respectively. The catalysts were found to be capable catalysts, indicating that wet impregnation might have left some Fe(III), Ni(II) on the accessible sites of SBA-15, which are responsible for converting more reactants. The UV-vis measurement spectra of bisphenol A degradation by catalysts **Fe/SBA-15**, **Ni/SBA-15** or **Fe-Ni/SBA-15** is shown in Figure 7. The absorbance peak became weaker in intensity with time and totally disappeared after 110 min, 100 min and 80 min with the catalysts **Fe/SBA-15**, **Ni/SBA-15** and **Fe-Ni/SBA-15**, respectively. This indicates that the bisphenol A was degraded totally into its mineral components. Similar results were reported by Fenton and sono-Fenton bisphenol A degradation by Ioan *et al.* (2007),³¹ but they did not report the final products of the reaction. In our work, the products of the catalytic degradation of bisphenol A were monitored by GC-MS analysis also (Scheme 1).

Effect of pH for Leaching Experiment: As the catalysts **Fe/SBA-15**, **Ni/SBA-15** and **Fe-Ni/SBA-15** contain transition metal ions (Fe^{3+} , Ni^{2+}), it is important to see whether they cause secondary pollution after use. The leaching of the metals from the catalysts was studied by vigorously agitating 0.1 g of the catalysts with 50 mL water at pH 3.0, 4.0, 5.0, 6.0, 7.0, 8.0, and 9.0 at 298 K (the temperature at which the wet oxidation reactions were carried out) for 2 h. The mixture was centrifuged and the amounts of Fe and Ni in the aqueous layer were determined. Fe released by **Fe/SBA-15** was between 0.50 and 1.18%, Ni released by **Ni/SBA-15** was from 0.03 and 0.14 % and from **Fe-Ni/SBA-15** catalyst 0.25 to 0.99% (Fe) and 0.01 to 0.12% (Ni), respectively.

The pH of the medium has significant influence on the leaching, but it was found that maximum release occurred at basic medium. The leaching in general is very small and does not give rise to concentration of the metals in water, which are higher than the permissible values even when drinking water quality is considered. The leachability experiment has shown that the amount of Fe and Ni released into

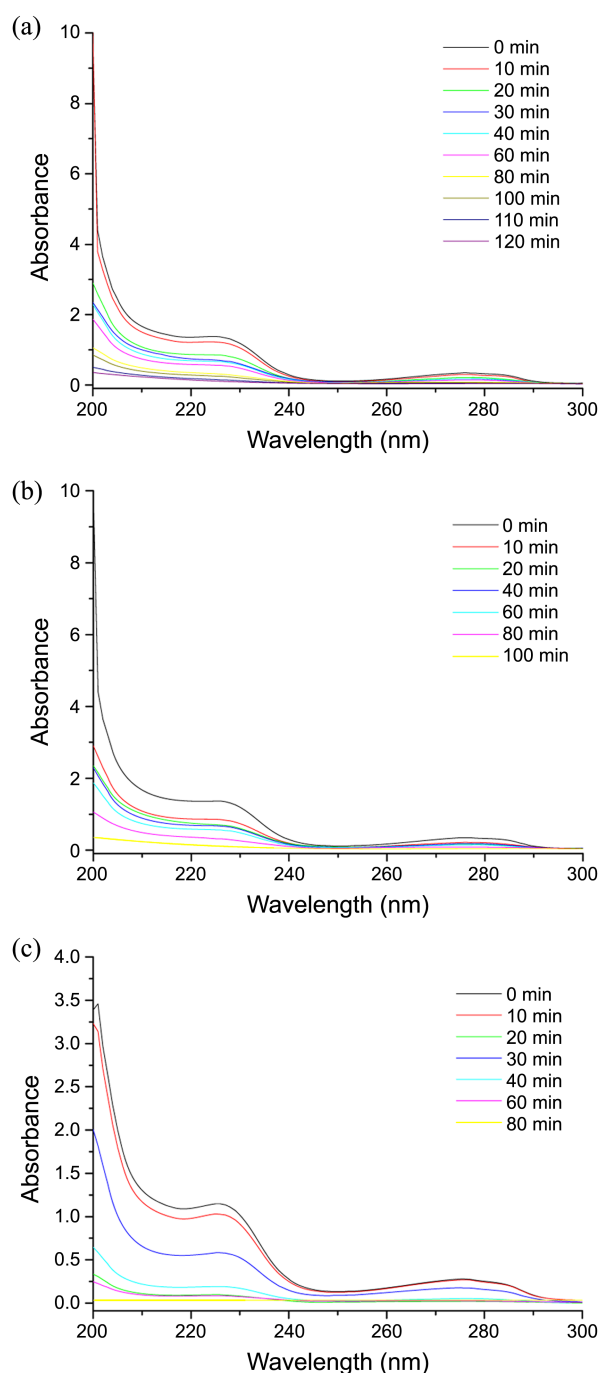
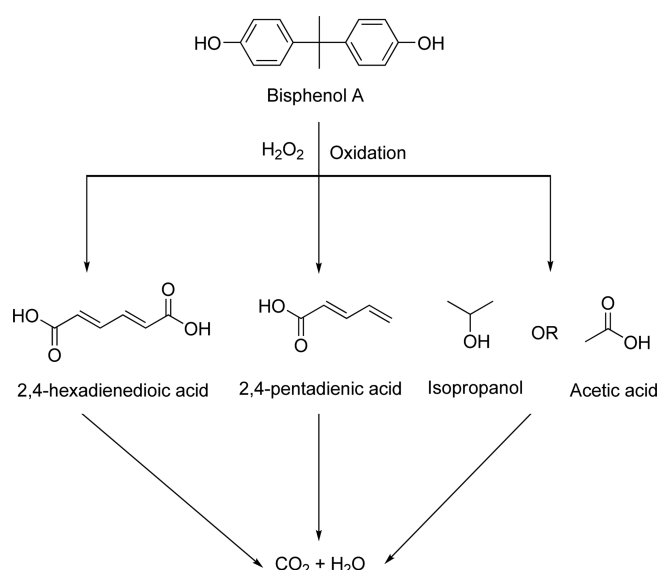


Figure 7. Time dependant UV-vis spectra of bisphenol A solutions with **Fe/SBA-15** (a), **Ni/SBA-15** (b) and **Fe-Ni/SBA-15** (c). Reaction conditions: bisphenol A $5 \times 10^{-4} \text{ mole L}^{-1}$, load 2 g L^{-1} , temperature 298 K.

water will give rise to a concentration of Fe and Ni far below the World Health Organization guideline³² value (for Fe(III) in natural fresh water ranges from 0.5 to 50 mg L^{-1} and for Ni in drinking water 0.02 mg L^{-1}). Thus, the use of the catalysts is not likely to create problem of water contamination.

Effect of Temperature: Although most of the experiments in this work were done at 298 K (close to room temperature), separate sets of experiments were designed to



Scheme 1. Main degradation pathways of bisphenol A during wet catalytic oxidation.

look into the effect of increasing temperature on bisphenol A degradation. Very small increase in the degradation was observed (Table 2) as the reaction was run successively at 288, 298, 303, 308 and 313 K. The increase in the degradation efficiency of the catalysts are evidently due to increased mobility of the bisphenol A molecules at higher temperature as well as their improved diffusional transport from the bulk phase to the liquid-catalyst interface. The oxidative degradation of bisphenol A with the catalysts, **Fe/SBA15**, **Ni/SBA15** and **Fe-Ni/SBA-15** were enhanced from 94.0-95.0%, 89.6-90.7% and 98.1-99.4%, respectively as the reaction was carried out at 288 K and 313 K. Similar trends were observed by Tang *et al.* (2011)⁷ in catalytic removal of bisphenol A from aqueous solution with hemoglobin immobilized on amino modified magnetic nano particles as an enzyme catalyst.

Product Analysis. The identification of reaction products from the wet catalytic oxidation of BPA was carried out with metal impregnated SBA-15 catalysts by means of the GC-MS analytical method (Scheme 1). The mechanism is based on $\cdot\text{OH}$ radicals. These radicals have their origin either in metal oxides formed during calcination of the catalysts or in the breaking of hydrogen peroxide (or water) molecules

Table 2. Effects of reaction temperature on catalytic oxidation of bisphenol A with **Fe/SBA-15**, **Ni/SBA-15** and **Fe-Ni/SBA-15** (load 2 g L^{-1} , bisphenol A: $5 \times 10^{-4} \text{ mole L}^{-1}$)

Temperature (K)	Conversion (%)		
	Fe/SBA-15	Ni/SBA-15	Fe-Ni/SBA-15
288	94.0	89.6	98.1
298	94.4	90.0	99.0
303	94.5	90.2	99.2
308	94.8	90.4	99.4
313	95.0	90.7	99.4

Table 3. Main bisphenol A intermediates identified by GC-MS

Peak No.	m/z	Molecular weight	Molecular structure	Product names
1	59	60	<chem>CC(O)C</chem> or <chem>CC(=O)O</chem>	Isopropanol or acetic acid
2	97	98	<chem>OC(=O)/C=C/C=C</chem>	2,4-pentadienic acid
3	141	142	<chem>OC(=O)/C=C/C=C/C(=O)O</chem>	2,4-hexadienedioic acid
4	227	228	<chem>Oc1ccc(cc1)C(C)(C)c2ccc(O)cc2</chem>	Bisphenol A

under the influence of the transition metal cations. The formation of $\cdot\text{OH}$ radicals on the surface of the catalysts will follow from interactions between the excited O-atoms of the catalyst and H-atoms cleaved from the substrate or even water because the reactions were carried out in an aqueous solution. The participation of dissolved oxygen in $\cdot\text{OH}$ radical formation is unlikely because this will result in a drastic reduction in oxidation with increasing reaction temperature (consequent to a decrease in dissolved oxygen level).³³ GC-MS analysis identified the following: 2,4-hexadienedioic acid, 2,4-pentadienic acid and isopropanol or acetic acid (Table 3). Subsequent oxidation of these intermediate products led to CO_2 and H_2O .⁷

Recyclability of the Catalysts. An attempt was made to recycle the catalysts **Fe/SBA-15**, **Ni/SBA-15** or **Fe-Ni/SBA-15** after catalytic oxidation of bisphenol A under the optimized reaction conditions. After the first catalytic reaction in the presence of H_2O_2 , the catalyst was isolated by filtration and the solid mass was Soxhlet-extracted with ethanol and water. The recovered solid was then dried in a vacuum desiccator overnight and used directly as catalyst in the next catalytic reaction. Four catalytic runs were carried out successfully with the same catalyst with no observable loss in performance (Figure 8).

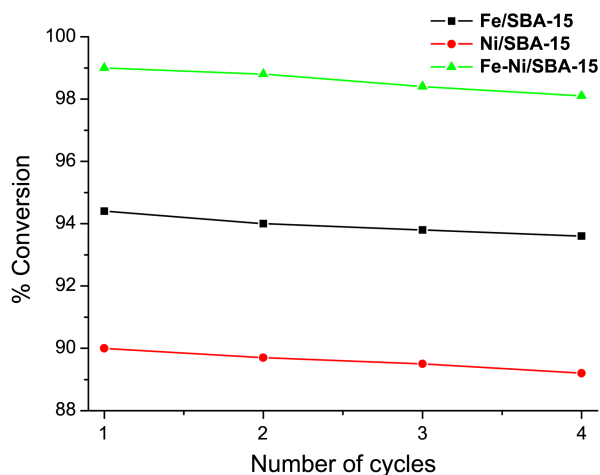


Figure 8. Efficiency of the catalysts, **Fe/SBA-15**, **Ni/SBA-15** and **Fe-Ni/SBA-15** in four consecutive cycles of bisphenol A oxidation.

Conclusion

We have demonstrated the successful immobilization of transition metals, iron and nickel onto SBA-15 materials to form **Fe/SBA-15**, **Ni/SBA-15** and **Fe-Ni/SBA-15** catalysts. SBA-15 itself is catalytically inactive, but the introduction of transition metals to SBA-15 can convert the material into an efficient oxidative catalyst for treating water contaminated with bisphenol A. According to the proposed breakdown pathway and the intermediates, the catalytic removal of bisphenol A by metal supported SBA-15 is considered to be an effective method. The degradation products identified were not persistent pollutants. GC-MS analysis identified the products: 2,4-hexadienedioic acid, 2,4-pentadienic acid and isopropanol or acetic acid. The recyclability of the catalyst was another advantage of the catalytic oxidative degradation process. The leaching experiment showed that iron, nickel metals did not create any new water pollution problems.

Acknowledgments. This study was supported by the National Research Foundation of Korea (NRF) grant funded by the Korea Government (MSIP) (NRF-2014M2B2A4030770) and Dongguk University–Gyeongju Research Fund.

References

- Xu, J.; Tang, T.; Zhang, K.; Ai, S.; Du, H. *Process Biochem.* **2011**, *46*, 1160-1165.
- Fu, P.; Zhang, P. *App. Catal. B: Environ.* **2010**, *96*, 176-184.
- Suzuki, N.; Hattori, A. *Life Sci.* **2003**, *73*(17), 2237-2247.
- Nakagawa, Y.; Tayama, S. *Arch. Toxicol.* **2000**, *74*(2), 99-105.
- Gupta, V. K.; Ali, I.; Saini, V. K. *Environ. Sci. Technol.* **2004**, *38*, 4012-4018.
- Jain, A. K.; Gupta, V. K.; Jain, S.; Suhas. *Environ. Sci. Technol.* **2004**, *38*, 1195-1200.
- Tang, T.; Fan, H.; Ai, S.; Han, R.; Qiu, Y. *Chemosphere* **2011**, *83*, 255-264.
- Jardim, W. F.; Moraes, S. G.; Takiyama, M. M. K. *Water Res.* **1997**, *31*, 1728-1732.
- Danis, T. G.; Albanis, T. A.; Petrakis, D. E.; Promonis, P. J. *Water Res.* **1998**, *32*(2), 295-302.
- Glaze, W. H.; Kang, J. W.; Chapin, D. H. *Ozone-Sci. Eng.* **1987**, *9*, 335-352.
- Beck, J. S.; Vartuli, J. C.; Roth, W. J.; Leonowicz, M. E.; Kresge, C. T.; Schmitt, K. D.; Chu, C. T.-W.; Olson, D. H.; Sheppard, E. W.; McCullen, S. B.; Higgins, J. B.; Schlenker, J. L. *J. Am. Chem. Soc.* **1992**, *114*, 10834-10843.
- Zhao, D.; Huo, Q.; Feng, J.; Chmelka, B. F.; Stucky, G. D. *J. Am. Chem. Soc.* **1998**, *120*, 6024-6036.
- Mayani, S. V.; Mayani, V. J.; Kim, S. W. *Canad. J. Chem. Eng.* **2013**, *91*(7), 1270-1280.
- Liu, H.; Li, Y.; Wu, H.; Takayama, H.; Miyake, T.; He, D. *Catal. Comm.* **2012**, *28*, 168-173.
- Zhao, D.; Feng, J.; Huo, Q.; Melosh, N.; Fredrickson, G. H.; Chmelka, B. F.; Stucky, G. D. *Science* **1998**, *279*, 548-552.
- Vinu, A.; Sawant, D. P.; Ariga, K.; Hossain, K. Z.; Halligudi, S. B.; Hartmann, M.; Nomura, M. *Chem. Mater.* **2005**, *17*, 5339-5345.
- Selvaraj, M.; Kawi, S. *Chem. Mater.* **2007**, *19*, 509-519.
- Liu, H.; Wang, H.; Shen, J.; Sun, Y.; Liu, Z. *Catal. Today* **2008**, *131*, 444-449.
- Hu, L.; Yang, X.; Dang, S. *App. Catal. B: Environ.* **2011**, *102*, 19-26.
- Calleja, G.; Melero, J. A.; Martinez, F.; Molina, R. *Water Res.* **2005**, *39*, 1741-1750.
- Busuioc, A. M.; Meynen, V.; Beyers, E.; Mertens, M.; Cool, P.; Bilba, N.; Vansant, E.F. *Appl. Catal. A: General* **2006**, *312*, 153-164.
- Melero, J. A.; Martinez, F.; Botas, J. A.; Molina, R.; Pariente, M. I. *Water Res.* **2009**, *43*, 4010-4018.
- Shukla, P.; Wang, S.; Sun, H.; Ang, H.-M.; Tade, M. *Chem. Eng. J.* **2010**, *164*, 255-260.
- Imamura, S. *Ind. Eng. Chem. Res.* **1999**, *38*, 1743-1753.
- Brieler, F. J.; Grundmann, P.; Froba, M.; Chen, L.; Klar, P. J.; Heimbrodt, W.; Nidda, H. A. K. V.; Kurz, T.; Loidl, A. *J. Am. Chem. Soc.* **2004**, *126*, 797-807.
- Huang, R.; Yan, H.; Li, L.; Deng, D.; Shu, Y.; Zhang, Q. *Appl. Catal. B: Environ.* **2011**, *106*, 264-271.
- Jung, H.; Kim, J.-W.; Cho, Y.-G.; Jung, J.-S.; Lee, S.-H.; Choi, J.-G. *Appl. Catal. A: General* **2009**, *368*, 50-55.
- Chiang, H.-L.; Wu, T.-N.; Ho, Y.-S.; Zeng, L.-X. *J. Hazard. Mater.* **2014**, *276*, 43-51.
- Calles, J. A.; Carrero, A.; Vizcaino, A. J. *Microporous Mesoporous Mater.* **2009**, *119*, 200-207.
- Zhao, M.; Church, T. L.; Harris, A. T. *Appl. Catal. B: Environ.* **2011**, *101*, 522-530.
- Ioan, I.; Wilson, S.; Lundanes, E.; Neculai, A. *J. Hazard. Mater.* **2007**, *142*, 559-563.
- WHO, *Guidelines for Drinking-Water Quality*, 3rd ed.; 1: Recommendations, World Health Organization, Geneva, 2004.
- Stoyanova, M.; Christoskova, St.; Georgieva, M. *Appl. Catal. A: General* **2003**, *249*, 295-302.